LBL-35273
UC-800

Lawrence Berkeley Laboratory
UNIVERSITY OF CALIFORNIA

EARTH SCIENCES DIVISION

Numerical Simulation of Coupled Flow and Transport with TOUGH2: A Verification Study

C.M. Oldenburg and K. Pruess

October 1994

U. C. Lawrence Berkeley Laboratory
Library, Berkeley

FOR REFERENCE

Not to be taken from this room

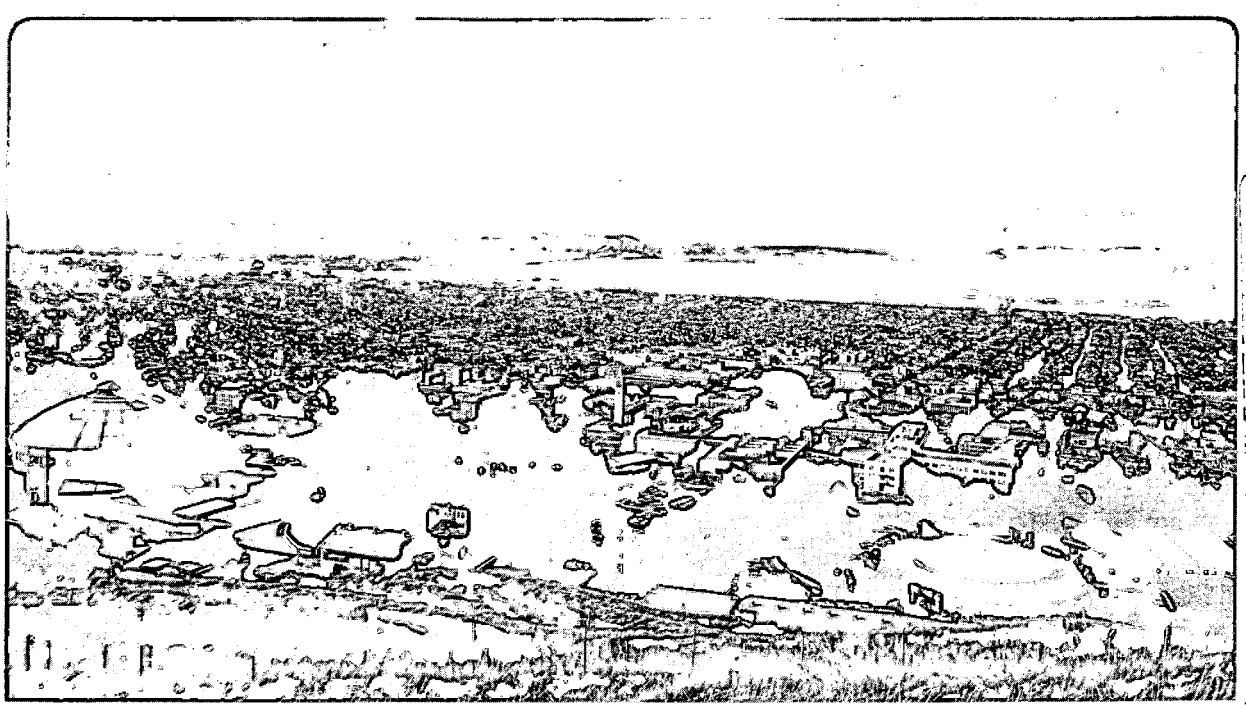

REFERENCE COPY
Does Not
Circulate
Bldg. 50 Library.
LBL-35273
Copy 1

Prepared for the U.S. Department of Energy under Contract Number DE-AC03-76SF00098

DISCLAIMER

This document was prepared as an account of work sponsored by the United States Government. While this document is believed to contain correct information, neither the United States Government nor any agency thereof, nor the Regents of the University of California, nor any of their employees, makes any warranty, express or implied, or assumes any legal responsibility for the accuracy, completeness, or usefulness of any information, apparatus, product, or process disclosed, or represents that its use would not infringe privately owned rights. Reference herein to any specific commercial product, process, or service by its trade name, trademark, manufacturer, or otherwise, does not necessarily constitute or imply its endorsement, recommendation, or favoring by the United States Government or any agency thereof, or the Regents of the University of California. The views and opinions of authors expressed herein do not necessarily state or reflect those of the United States Government or any agency thereof or the Regents of the University of California.

LBL-35273

Numerical Simulation of Coupled Flow and Transport with TOUGH2: A Verification Study

Curtis M. Oldenburg and Karsten Pruess

Earth Sciences Division
Lawrence Berkeley Laboratory
University of California
Berkeley, CA 94720

October 1994

This work was supported by the WIPP project, Sandia National Laboratories, under Document No. 129847, through the U.S. Department of Energy, under contract No. DE-AC03-76SF00098

Abstract

We have tested T2DM, the dispersion module of TOUGH2, on two classic flow problems: (1) the seawater intrusion problem of Henry (1964); and (2) the pure solutal free convection problem of Elder (1967). T2DM produces results in agreement with prior work for similar spatial discretizations. In the Henry problem, finer spatial discretization allows the seawater tongue to penetrate slightly farther without affecting the overall flow dynamics. In the strongly coupled pure solutal free convection problem of Elder, results produced by T2DM using high-resolution grids differ markedly from lower-resolution results. These high-resolution simulations agree closely with laboratory experiments.

Contents

1. Introduction 4

2. Henry Problem 5

3. Elder Problem 7

4. Conclusions 9

References 10

Acknowledgments 11

Nomenclature 12

List of Figures

Fig. 1. Domain and results for the Henry seawater intrusion problem 15

Fig. 2. Finer discretizations for the Henry problem 16

Fig. 3. Results for the Henry problem on finer grid 17

Fig. 4. Henry problem with pure hydrodynamic dispersion 18

Fig. 5. Domain for the Elder free-convection problem 19

Fig. 6. Calculated results of the Elder free-convection problem 20

Fig. 7. Experimental results of Elder 21

Fig. 8. Finer discretizations for the Elder problem 22

Fig. 9. High-resolution results for the Elder problem 23

List of Tables

Table 1. Parameters for the Henry problem 13

Table 2. Parameters for the Elder problem 14

1. Introduction

We have recently implemented full hydrodynamic dispersion for two-dimensional flow and transport in our general-purpose simulator TOUGH2 (Pruess, 1987; Pruess, 1991; Oldenburg and Pruess, 1993). With the goal of verifying the dispersion module (T2DM), we follow the suggestion of Voss and Souza (1987) who recommend comparing calculated results for two classic coupled flow problems. These are (1) the seawater intrusion problem of Henry (1964) and (2) the free convection problem of Elder (1967). These problems involve coupling between the flow and transport because the density is controlled by solute concentration. The Henry problem involves density variations of only about 2.5%, while the Elder problem has density variations of 20%. This makes the Elder problem a strongly coupled flow problem. Many numerical solutions have been presented for both of these problems through the years. The agreement between our calculated results and other models serves to verify T2DM. The context for the present verification study is presented in detail in Oldenburg and Pruess (1995). Details on the theory and implementation of dispersive transport in T2DM are presented in Oldenburg and Pruess (1993).

Both of the test problems presented here are pure molecular diffusion problems and do not involve hydrodynamic dispersion. In a prior report (Oldenburg and Pruess, 1993), we presented a comparison between calculated results and the analytical solution for a problem of two-dimensional transport with hydrodynamic dispersion of a tracer introduced into a homogeneous, isotropic, saturated porous medium with a steady-state flow field. The analytical solution for this problem was given in Javandel et al. (1984). Although the tracer concentration does not affect the flow field, tracer transport is coupled to the flow field through the velocity dependence of dispersion. Good agreement with the analytical result was observed. In the absence of hydrodynamic dispersion, the coupling between the solute transport and the flow equations arises through the density

dependence of the fluid on the solute concentration. This is the relevant coupling in the test problems of the present study.

2. Henry Problem

The Henry problem is a seawater intrusion problem presented by Henry (1964). As such, it involves total density variations of only 2.5%. The problem considers a two-dimensional cross-section with constant flow of fresh water ($X_b = 0.$) from the left-hand side to the right-hand side on which the concentration is set to be that of seawater ($X_b = 1.$) and the pressure is set as hydrostatic assuming seawater density. This problem of rather modest density variation is tractable by many methods and models. The parameters for the problem as discussed in Voss and Souza (1987) are given in Table 1. The T2DM calculation is performed with the option MOP(13) = 0. For the purposes of calculating dispersive fluxes, this option interpolates components of the velocity and concentration gradient vectors assuming these vectors are zero at the boundaries of the domain. We also set MOP(18) = 0 for full upstream weighting of density at grid block interfaces. We have set the tortuosity of the right-hand boundary column (Fig. 1) equal to zero so that the diffusive flux of brine is zero into or out of this boundary. Boundary conditions and results at steady state from T2DM and SUTRA (Voss, 1984) as reported in Voss and Souza (1987) are presented in Fig. 1. We observe a brine tongue penetrating from right to left under the main left to right flow of fresh water. Penetration of the seawater tongue occurs due to the density contrast between the seawater and the fresh water. T2DM performs very efficiently on this coupled problem. With an initial time step size of 100 seconds, it takes 22 time steps to get to a total time of 4.5×10^7 seconds; there is little change in the solution after about 10^6 seconds. Reasonable agreement with Voss and Souza (1987) is observed for a comparable spatial discretization, indicated by the 0.1 m square grid blocks shown in Fig. 1. It appears that Voss and Souza (1987) neglected the right-hand boundary value of concentration ($X_b = 1$) in their plotting of

concentration isopleths. The results of Voss and Souza (1987) are representative of the many results obtained by other researchers using other codes.

To test whether the discrepancies of the $X_b = .25$ and .75 isopleths between our calculated results and those of Voss and Souza (1988) were due to excessive numerical diffusion in T2DM, we performed a limited grid-resolution study. Two finer discretizations are shown in Fig. 2. Results for the calculations using the finer discretizations are shown in Fig. 3. T2DM requires more time steps with finer grids. With an initial time-step size of 100 seconds, the 0.05 meter-grid block discretization took 21 time steps to get to a total time of 2.3×10^7 seconds. With an initial time-step size of 10 seconds for the 0.025 meter-grid block mesh took 27 time steps to get to a total time of 9.1×10^6 seconds. Grid effects are seen to be small. We note that the diminished numerical diffusion associated with the finer grids results in slightly greater penetration of the seawater tongue at the bottom. This occurs because the density contrast between the tongue and the fresh water is better maintained when numerical diffusion is smaller. Nevertheless, the flow dynamics and overall concentration fields are very similar. Differences between results and those of Voss and Souza (1987) may be due to small differences in boundary conditions and parameter values.

For the purposes of comparison, we present next the Henry problem with velocity-dependent dispersivity. In order to approximate the pure molecular diffusion case of the actual Henry problem, we choose dispersivities that will give rise to approximately the same effective diffusivity as in the actual Henry problem. Specifically, with a mass source (Q) equal to 6.6×10^{-2} kg s^{-1} m^{-1} of fluid of density 1×10^3 kg m^{-3} entering along the 1 m-high left-hand side boundary (h) with 1 m^2 area (A), a typical Darcy velocity would be 6.6×10^{-5} m s^{-1} (i.e., $u = Q\,h / A\,\rho$). The original Henry problem specified molecular diffusivity (d) of 6.6×10^{-6} m^2 s^{-1} which is approximately equivalent to dispersivities (α_L, α_T) of .035 m for porosity (ϕ) equal to .35 (i.e., $u\,\alpha = \phi\,d$). The steady state result using $d = 0.$ and $\alpha_L = \alpha_T = .035$ m is presented in Fig. 4. Note

the overall similarity of the results in Figs. 3 and 4, consistent with the choice of dispersivities. Nevertheless, the shape of the salinity isopleths differs slightly. The greater curvature of the isopleths is due to (a) the greater penetration of the brine tongue along the bottom where velocities are lower and hence dispersive fluxes are lower, and (b) the larger dispersive fluxes associated with larger velocities in the upper regions of the domain. This same effect was seen in the study of Frind (1982) for velocity-dependent dispersivity. The non-zero brine mass fraction in the upper right-hand corner is due to upstream dispersive fluxes from the right-hand side boundary (deMarsily (1986), p. 242–243).

3. Elder Problem

The Elder problem is a free-convection problem originally conceived as being pure thermal convection with heating from below, but easily adapted for pure solutal convection with a salt source at the top. The large maximum density change (20%) makes this a strongly coupled flow problem. Because Elder performed experiments in a Hele-Shaw cell and was interested in thermal convection, the emphasis in this problem is on the coupled nature of the flow rather than hydrodynamic dispersion. As in the Henry problem, transport is by advection and pure molecular diffusion rather than velocity-dependent hydrodynamic dispersion.

Elder (1967) used dimensionless space and time in his calculations. His laboratory apparatus was a Hele-Shaw cell 5 cm by 20 cm. We use physical dimensions and parameters scaled to match Elder's work and apparently chosen by Voss and Souza. These parameters are presented in Table 2. The domain, boundary conditions, and discretization for the problem are presented in Fig. 5 (note the vertical exaggeration chosen to match plots in Voss and Souza (1987)). The emphasis of Elder's work was on transient convection and the results are not taken to steady state. As shown in Fig. 6, our calculated transient results agree with the calculated results of Elder (1967) and Voss and

Souza (1987) for a similar spatial discretization (Fig. 5). Note in particular that there are two cells with a central downwelling at the times indicated. This result is symmetric and we have verified that it is identical to calculations performed in one-half of the box and reflected about the mirror plane at Y = 300 m.

Elder (1967) presented photographic plates showing the flow field in the Hele-Shaw cell apparatus used in his thermal convection experiments. Elder's experimental apparatus had a height of 5 cm and length of 20 cm with a 10 cm-long heated region centered at the bottom. If the aspect ratio and depth of the Hele-Shaw cell are undistorted in the photograph, then the ends of the apparatus must have been cropped from the picture. We have inferred based on the flow field that this is the case. We show in Fig. 7 a reproduction of Elder's figure, turned upside down to correspond to our solutal convection scenario and embellished with the boundary condition and physical dimensions, along with approximate streamlines derived from the flow field. Note that the experimental result has a central upwelling while the calculated flow field of Fig. 6 has a central downwelling.

In order to investigate this lack of agreement between laboratory experiment and numerical simulation, we performed a grid resolution study that revealed the importance of the spatial discretization on the calculated results for the Elder (1967) problem. We show in Fig. 8 two finer discretizations (no vertical exaggeration) which take advantage of the symmetry of the problem. Fig. 9 shows the corresponding calculated results. The convection process begins with downward flow near the edge of the region where the X_b = 1.0 boundary condition is maintained. The t = 2 yrs. results show a single downwelling plume centered near Y = 130 m. Flow is upwards on both sides of this saline plume. With time, this region of downflow moves towards the center line (Y = 0). However, it does not actually reach the center line, and at later times in this transient flow there is upflow at the center line (Y = 0), which corresponds to central upwelling rather than central downwelling as found for the coarse discretization. In addition, note that

calculated results for the two discretizations of Fig. 8 are very similar. This indicates that we have achieved grid convergence, with the higher-resolution calculations bringing the low-resolution results (Fig. 6) into question. We note finally that our high-resolution results agree with the photograph of the experiment presented in Elder (1967) and reproduced here in Fig. 7. In particular, Elder's experiment showed upflow near the center with four convection cells. Our grid-resolved results agree well with Elder's in terms of the number of convection cells and the direction of circulation. These results show that there is a certain length scale for the convection cells that arises from the density difference and strength of diffusion at the brine source. This scale could not be resolved by the coarse grid, but is resolved by both of the fine grids of Fig. 8.

4. Conclusions

We have tested the dispersion module T2DM on two classic coupled flow problems. For discretizations similar to that of prior researchers, T2DM produces results that agree closely with prior work. For the case of modest density variation associated with the Henry seawater intrusion problem, the flow dynamics do not change significantly with finer discretization. The Elder problem on the other hand is sensitive to spatial discretization. Initial simulations with coarse spatial discretization agreed well with results from other codes. The grid-converged results are quite different from those obtained with coarse discretization. Our grid-converged results agree well with Elder's laboratory experiments.

References

Elder, J.W., Transient convection in a porous medium, *J. Fluid Mech.*, *27*(3), 609–623, 1967.

Frind, E.O., Simulation of long-term transient density-dependent transport in groundwater, *Adv. Water Resources*, *5*, pp. 73–88, June, 1982.

Henry, H.R., Effects of dispersion on salt encroachment in coastal aquifers, *U.S. Geol. Survey Water Supply Paper*, *1613-C*, C71–C84, 1964.

Javandel, I., Doughty, C., and Tsang, C.-F.,*Groundwater Transport, Handbook of Mathematical Models*, American Geophys. Union, pp. 14-19, 1984.

deMarsily, G., *Quantitative Hydrogeology*, Academic Press, New York, 440 pp., 1986.

Oldenburg, C.M. and Pruess, K., A two-dimensional dispersion module for the TOUGH2 simulator, *Lawrence Berkeley Laboratory Report*, *LBL- 32505*, Berkeley, California, 1993.

Oldenburg, C.M. and Pruess, K., Dispersive transport dynamics in a strongly coupled groundwater brine flow problem, *Water Res. Res, in press*, 1995.

Pruess, K., TOUGH User's Guide, Nuclear Regulatory Commission, Report NUREG/CR-4645, June 1987 (also *Lawrence Berkeley Laboratory Report*, *LBL-20700*, Berkeley, California, June 1987).

Pruess, K., TOUGH2 - A General Purpose Numerical Simulator for Multiphase Fluid and Heat Flow, *Lawrence Berkeley Laboratory Report*, *LBL-29400*, Berkeley, California, May 1991).

Voss, C.I., SUTRA: A finite-element simulation model for saturated-unsaturated fluid-density-dependent ground-water flow with energy transport or chemically-reactive single-species solute transport, *U.S. Geol. Surv. Water-resour. Invest. Rep.*, 84-4369, 409 pp., 1984.

Voss, C.I., and Souza, W.R., Variable density flow and solute transport simulations of regional aquifers containing a narrow freshwater-saltwater transition zone, *Water Res. Res.*, *23*(10), 1851–1866, 1987.

Acknowledgments

This work was supported by the WIPP project, Sandia National Laboratories, through the U.S. Department of Energy, under contract No. DE–AC03–76SF00098. We thank Steve Webb, Sandia National Laboratories, for helpful discussion throughout the course of the work. Thanks are also due to Emilio Antunez and Stefan Finsterle for thoughtful reviews of an earlier draft.

Nomenclature

A	area	m^2
d	molecular diffusivity	$m^2\ s^{-1}$
h	left-hand side boundary height	m
k	permeability	m^2
Q	mass source	$kg\ s^{-1}\ m^{-1}$
t	time	years
X	mass fraction	
Y	Y-coordinate	
Z	Z-coordinate (positive upward)	

Greek symbols

α	intrinsic dispersivity	m
μ	dynamic viscosity	$kg\ m^{-1}\ s^{-1}$
ϕ	porosity	
ρ	density	$kg\ m^{-3}$
τ	tortuosity	

Subscripts and superscripts

b	brine
in	injection
L	longitudinal
0	reference value
T	transverse

Table 1. Parameters for the Henry (1964) problem.

symbol	quantity	value	units
ϕ	porosity	.35	–
k	permeability	1.02×10^{-9}	m^2
μ	viscosity	1.0×10^{-3}	Pa s
g	gravity	9.81	$m\ s^{-2}$
α_T	transverse dispersivity	0., .035	m
α_L	longitudinal dispersivity	0., .035	m
d	molecular diffusivity	6.6×10^{-6}	$m^2\ s^{-1}$
τ	tortuosity	1.	–
ρ_0	density of pure water	1000.	$kg\ m^{-3}$
ρ_b	density of pure brine	1025.	$kg\ m^{-3}$
P(0 m)	pressure on right boundary	hydrostatic for pure brine	
Q	mass source on left side	6.6×10^{-2}	$kg\ s^{-1}\ m^{-1}$

Table 2. Parameters for the Elder (1967) problem.

symbol	quantity	value	units
ϕ	porosity	.1	–
k	permeability	4.845×10^{-13}	m^2
μ	viscosity	1.0×10^{-3}	Pa s
g	gravity	9.81	$m\ s^{-2}$
α_T	transverse dispersivity	0.	m
α_L	longitudinal dispersivity	0.	m
d	molecular diffusivity	3.565×10^{-6}	$m^2\ s^{-1}$
τ	tortuosity	1.	–
ρ_0	density of pure water	1000.	$kg\ m^{-3}$
ρ_b	density of pure brine	1200.	$kg\ m^{-3}$

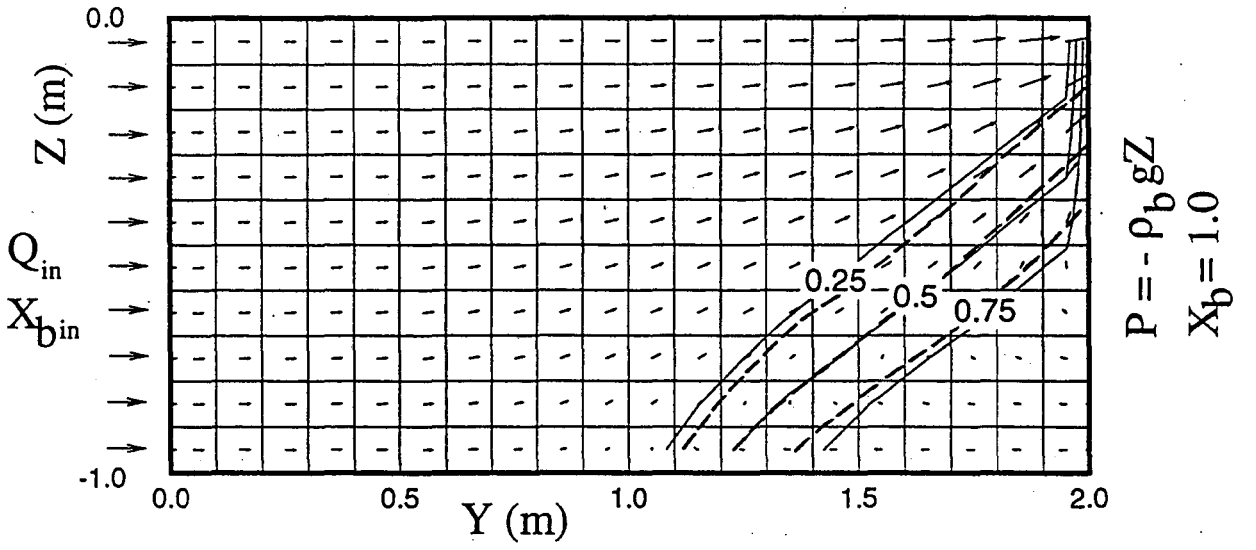

Fig. 1. Domain, boundary conditions and steady-state results for the Henry (1964) seawater intrusion problem with 0.1 m square grid blocks. The contours are lines of constant brine mass fraction. The flow field is shown by the vectors, with Darcy velocity in the left-most column of grid blocks equal to approximately 6.6×10^{-5} m s^{-1}. Dashed line is result of Voss and Souza (1988). Solid line is from T2DM.

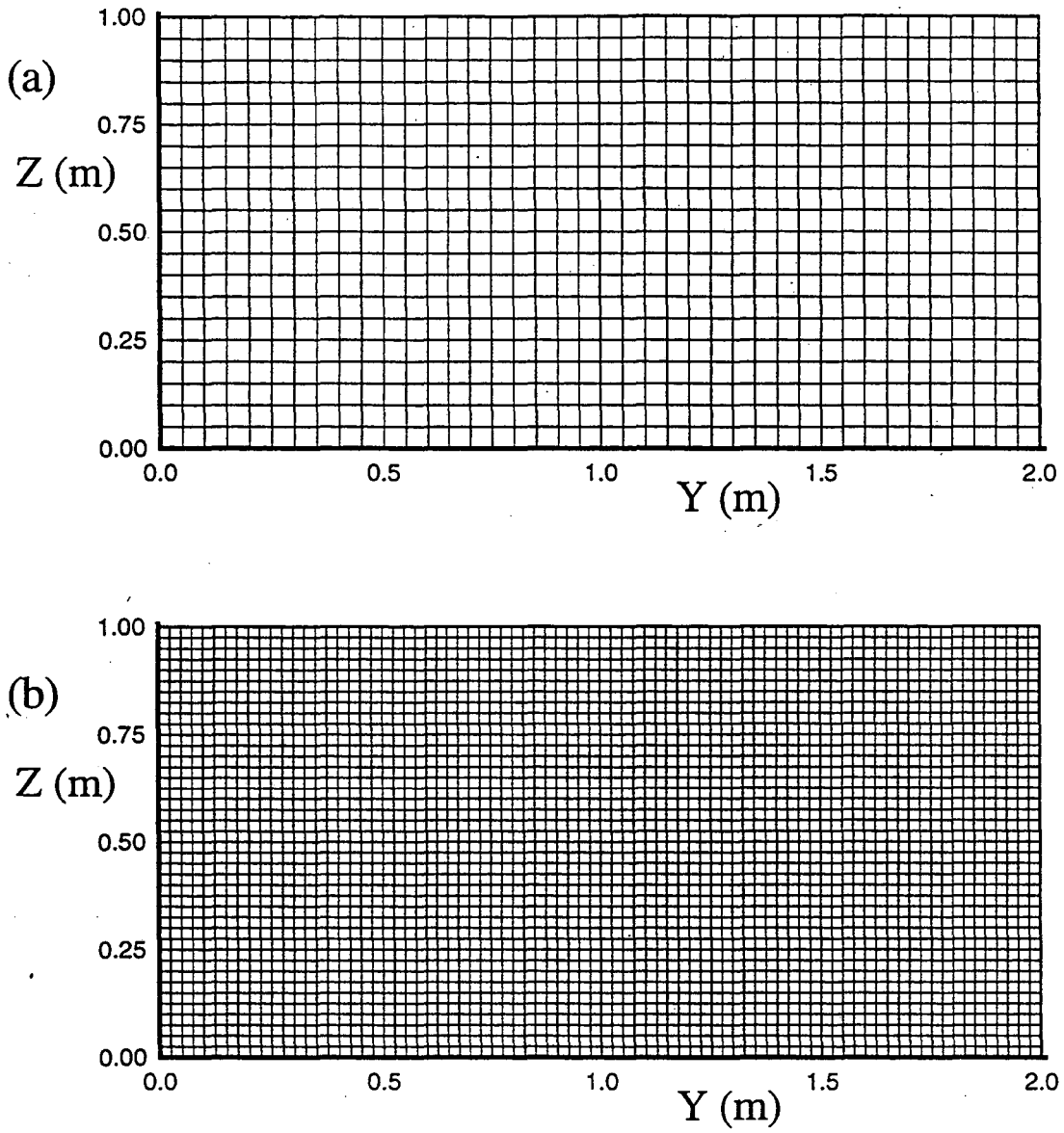

Fig. 2. Two finer discretizations for the Henry (1964) seawater intrusion problem. (a) 0.05 m square grid blocks; (2) 0.025 m square grid blocks.

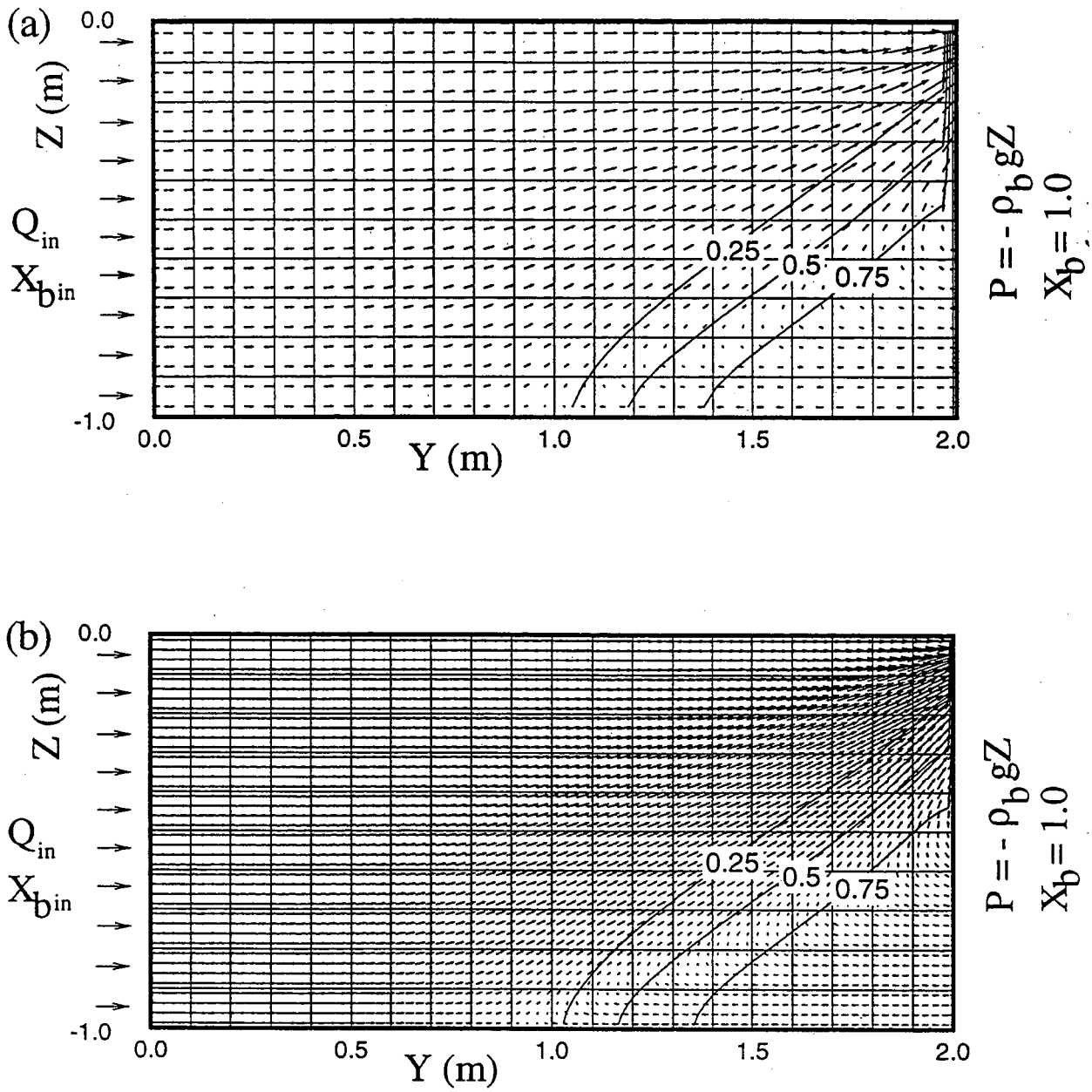

Fig. 3. Results for the Henry (1964) problem calculated on the finer grids. (a) 0.05 m square grid; (b) 0.025 m square grid. Note the slight differences in the length of the seawater tongue depending on grid block size. The flow field is shown by the vectors, with Darcy velocity in the left-most column of grid blocks equal to approximately 6.6 x 10^{-5} m s^{-1}.

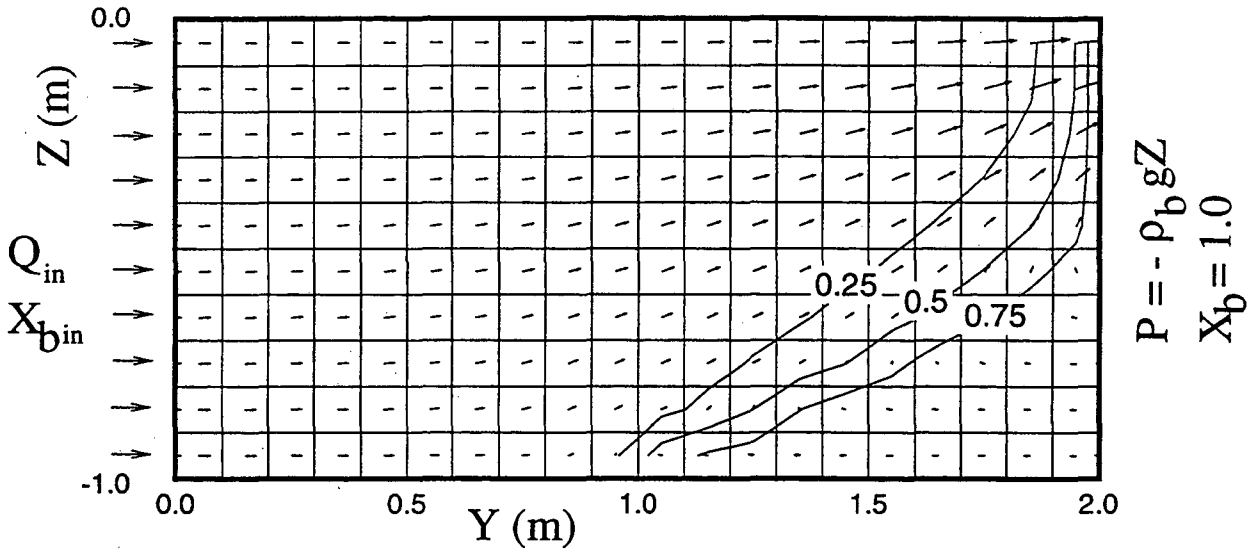

Fig. 4. Results for the Henry (1964) problem calculated on the coarse grid with $d = 0.$ m^2 s^{-1} and $\alpha_T = \alpha_L = .035$ m. Note the differences in the shape of the brine isopleths between Fig. 4 and Figs. 1 and 3. The flow field is shown by the vectors, with Darcy velocity in the left-most column of grid blocks equal to approximately 6.6×10^{-5} m s^{-1}.

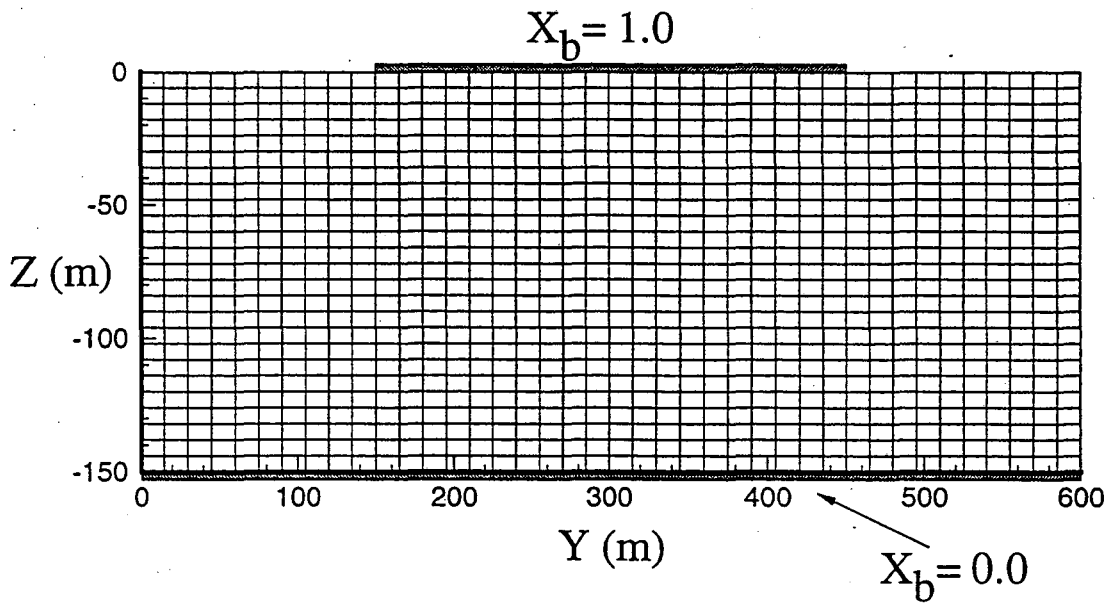

Fig. 5. Domain, boundary conditions and discretization for the free convection problem of Elder (1967). Note the vertical exaggeration in accordance with the presentation of Voss and Souza (1987).

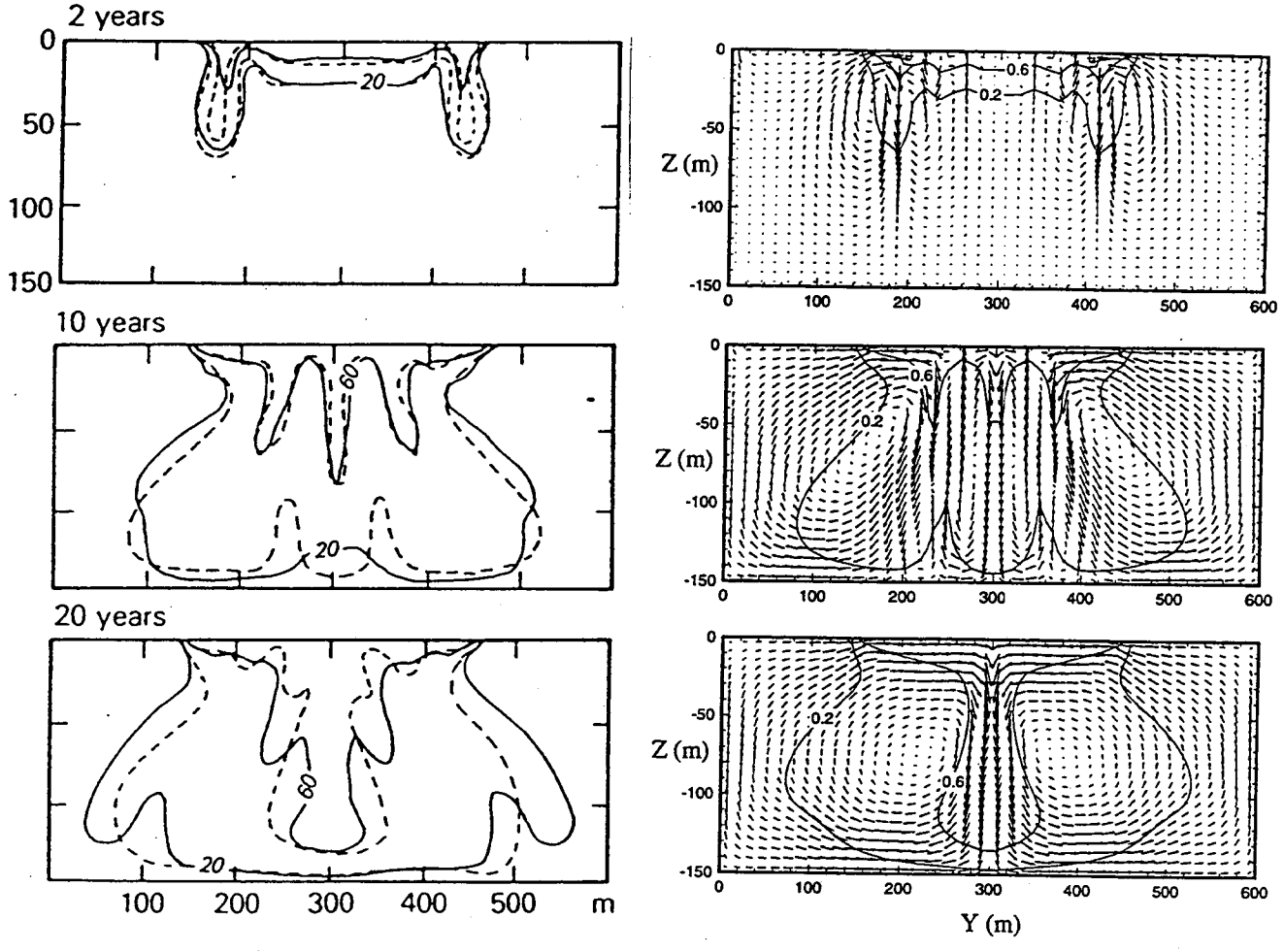

Fig. 6. Results of the Elder (1967) free-convection problem at 2, 10, and 20 years. Left-hand column, results of Elder (1967) (dashed lines) and Voss and Souza (1987) (solid lines). Contour lines are labeled as fraction of maximum solute concentration in percent. Right-hand column, fluid velocity and isopleths of concentration calculated using the current model. Contour lines are labeled as mass fraction of maximum solute concentration ($X_{b,max}$ = 1.0). Maximum Darcy velocity is approximately 2.0 x 10^{-7} m s^{-1}.

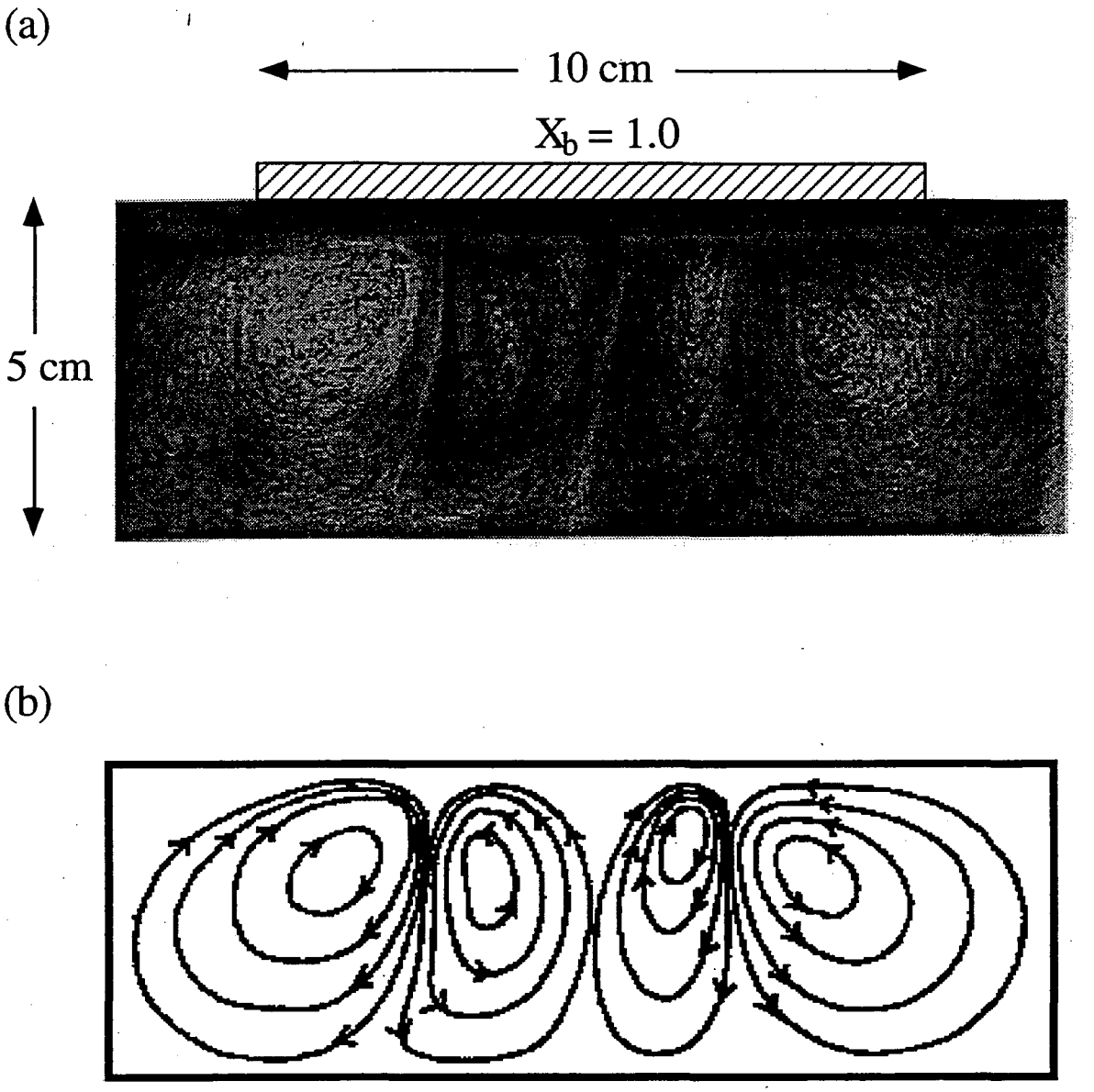

Fig. 7. Experimental results of Elder (1967): (a) flow visualization as presented by Elder and embellished with brine source boundary condition; (b) approximate streamlines shown for clarity.

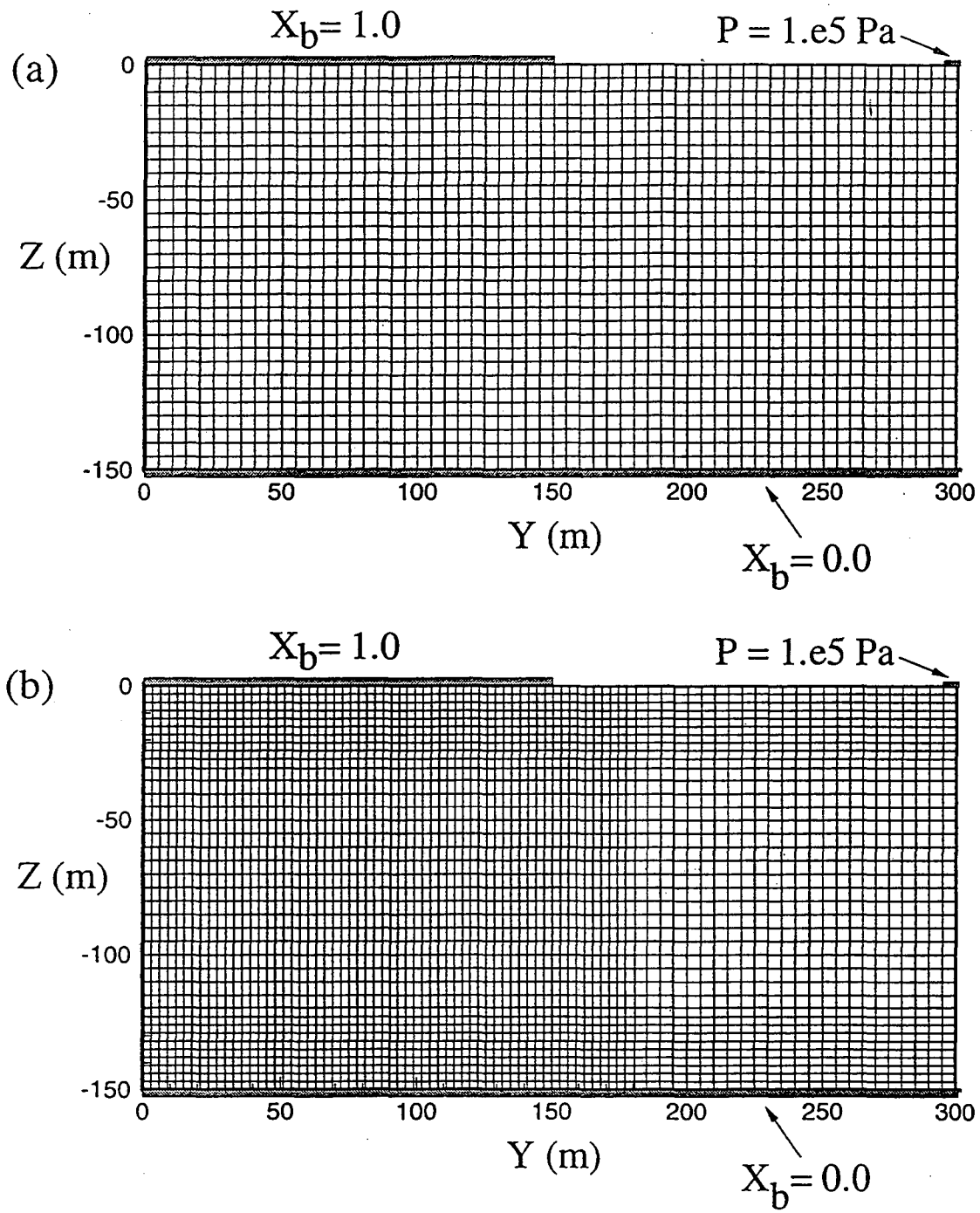

Fig. 8. Two finer discretizations for the Elder problem grid-resolution study (no vertical exaggeration) which take advantage of the symmetry of the problem. (a) uniform NX x NZ = 60 x 32 grid blocks; (b) graded 84 x 42. In both (a) and (b), the top and bottom rows of grid blocks are too narrow to appear in the figure.

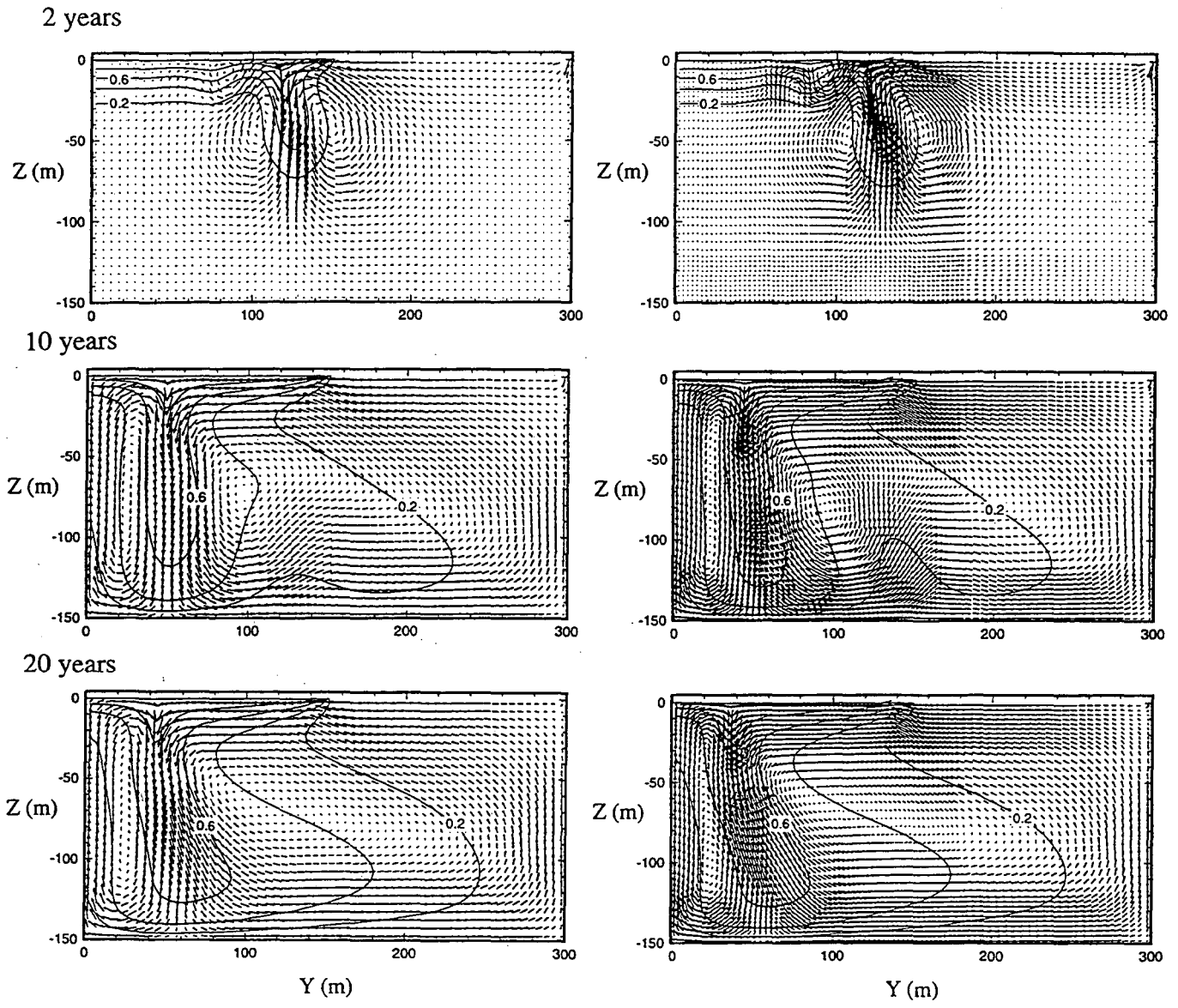

Fig. 9. High-resolution results for the Elder free-convection problem for the two different discretizations of Fig. 7 at $t = 2$, 10, and 20 years. Contours are labeled with mass fraction of maximum brine concentration ($X_{b,max} = 1.0$). Flow field and concentration isopleths show absence of central down-welling and multiple convection cells in agreement with the experimental results of Elder (1967) reproduced in Fig. 6. Maximum Darcy velocity is approximately 2.0×10^{-7} m s^{-1}.

LAWRENCE BERKELEY LABORATORY
UNIVERSITY OF CALIFORNIA
TECHNICAL INFORMATION DEPARTMENT
BERKELEY, CALIFORNIA 94720